Crystals **2015**, *5*, 302-311; doi:10.3390/cryst5030302

OPEN ACCESS

crystals

ISSN 2073-4352

www.mdpi.com/journal/crystals

Article

Pitch-Length Independent Threshold Voltage of Polymer/Cholesteric Liquid Crystal Nano-Composites

Hoekyung Kim, Junji Kobashi, Yasutaka Maeda, Hiroyuki Yoshida * and Masanori Ozaki

Department of Electrical, Electronic and Information Engineering, Osaka University, 2-1 Yamada-oka, Suita, Osaka 565-0871, Japan; E-Mails: hkim@opal.eei.eng.osaka-u.ac.jp (H.K.); jkobashi@opal.eei.eng.osaka-u.ac.jp (J.K.); ymaeda@opal.eei.eng.osaka-u.ac.jp (Y.M.); ozaki@eei.eng.osaka-u.ac.jp (M.O.)

* Author to whom correspondence should be addressed; E-Mail: yoshida@eei.eng.osaka-u.ac.jp; Tel.: +81-6-6879-7759; Fax: +81-6-6879-4838.

Academic Editor: Oleg D. Lavrentovich

Received: 3 July 2015 / Accepted: 13 August 2015 / Published: 19 August 2015

Abstract: Polymer/cholesteric liquid crystal (ChLC) nano-composites consisting of mesogenic monomers and LCs have nano-sized LC domains dispersed in an anisotropic polymer matrix. They exhibit characteristics not observed in conventional ChLCs, such as sub-millisecond and "deformation-free" electro-optic tuning of the selective reflection band; however, their driving voltage is high compared to conventional ChLCs, and is an issue that needs to be solved for the practical use. Here, we investigate the helical pitch dependence of threshold voltage in polymer/ChLC nano-composites. Five samples with different helical pitches were prepared and their electro-optic characteristics were compared before and after photopolymerization. Although the threshold voltage of the unpolymerized samples were inversely proportional to its helical pitch, the threshold voltage of the polymerized samples showed no dependence on the helical pitch. These results are explained to be a consequence of the driving mechanism of the polymer/ChLC nano-composite, in which electro-optic switching is achieved as a consequence of the nano-confined LC molecules reorienting along the electric field, instead of the helical structure becoming unwound. The threshold voltage is independent of pitch length because the pore sizes are similar in all samples.

Keywords: cholesteric liquid crystal; polymer/cholesteric liquid crystal nano-composite; polymer networks; helical pitch; threshold

1. Introduction

Cholesteric liquid crystals (ChLCs) are one-dimensional photonic band-gap materials in which the constituent LC molecules self-organize into a helical structure. They exhibit a so-called selective reflection band, in which light with the same circular handedness as the helix is reflected: the selective reflection band spans over the wavelength $n_o \times p - n_e \times p$, where n_e and n_o are the extraordinary and ordinary refractive indices and p is the helical pitch [1]. The helical pitch, p, is defined as the distance required for the director to twist by 2π. Therefore, the reflection band can be modulated by changing the helical pitch. Control of helical pitch by external stimuli, such as by electric field [2], temperature [3], pressure [4], and light irradiation [5,6], have been proposed. Among these methods, electric field tuning of the selective reflection band is the best choice for practical use because of its switching speed and compatibility with other electro-optic devices. Some previous reports have demonstrated applications, such as displays [7] and lasers [8,9], based on electro-optic switching of the selective reflection band.

Conventional ChLCs, however, are difficult to implement into electro-optic devices because the selective reflection band tuning is irreversible and slow. When increasing the external electric field, the helical structure of ChLC is destroyed at high electric fields. To overcome this intrinsic drawback, polymer stabilized ChLCs (PSChLCs) have been investigated intensively [10]. PSChLCs are obtained by dissolving a small amount of a photopolymerizable monomer (5~10 wt %) in a low-molecular weight ChLC and polymerizing the sample *in situ* in the Ch phase. Although this material shows improved reversibility with reduced switching times (~few ten ms), it still has drawbacks in that degradation of peak reflectance and broadening of selective reflection band-width occurs [11]. Moreover, the current switching time of PSChLCs still limits their use in electro-optic applications. Therefore, there is an urgent need to develop ChLCs with better structural stability and response times.

Recently, we have reported a polymer/ChLC nano-composite, which shows fast and deformation-free electro-optic tuning of the selective reflection band [12]. The polymer/ChLC nano-composites also comprise mesogenic monomers and ChLCs similar to PSChLCs, but they typically contain a higher concentration of monomer and show distinct properties; upon the application of an electric field, the macroscopic helical structure is retained, and only the LC molecules inside the nano-pores reorient along the electric field. Because of the high miscibility between the polymer and the liquid crystal, polymerization-induced phase separation is suppressed, and a porous polymer matrix possessing helical molecular orientation is obtained. The pores in the polymer matrix is typically on the order of several 10–100 nm, which is significantly smaller compared to PSChLCs, which have LC domains sizes of typically 400–500 nm [13,14]. Since the nano-pores are much smaller than the visible light wavelength, they do not give rise to scattering nor deform the helical structure, but affect the effective refractive index instead. Reorientation of the LC molecules within the nano-pores decreases the effective extraordinary refractive index of the nano-composite, leading to a shortening of the long selective reflection band-edge wavelength without affecting the short reflection band-edge. Combined with the fast response, which results from the LCs being confined in nano-sized pores, the proposed nano-composites open new possibilities for the application of ChLCs. However, further studies are needed to improve the properties of this material, because its driving electric field is high (several 10 V/μm) compared to conventional ChLCs.

Here, we investigate the helical pitch dependence of the threshold voltage in the polymer/ChLC nano-composite. Five samples with different helical pitches are prepared and their electro-optic properties are compared before and after polymerization. Interestingly, the threshold voltages of the nano-composites show little dependence on the pitch length, while the unpolymerized samples show a clear inversely proportional relationship with the pitch. We attribute this difference to the driving mechanism of the nano-composite, in which the threshold is determined by the pore-size, and to the fact that the polymer morphology of the nano-composites are similar despite having different pitch lengths.

2. Experimental Section

We prepared five types of mesogenic monomer/ChLC mixtures with different chiral dopant concentrations. The composition of each sample is listed in Table 1. The mesogenic monomer/ChLC mixtures comprised three materials from Merck: a photopolymerizable LC monomer (RM257); a nematic LC (MLC-6657-000); and a chiral dopant (ZLI-4572). No photo-initiator was used in this study. The physical properties of MLC-6657-000 and RM257 are listed in Table 2. The relative weight ratio of RM257 and MLC-6657-000 were set to 19.9 and 80.1, respectively and the chiral dopant ZLI-4572 was added to this mixture to change the helical pitch of the polymer/ChLC nano-composite. The chiral dopant concentration was varied from 6 to 10 wt %. The materials were dissolved in chloroform and left to evaporate for approximately 1 day.

Table 1. Compositions of the samples used in this study.

Sample ID	LC Monomer (RM257)	Nematic LC (MLC-6657-000)	Chiral Dopant (ZLI-4572)
Sample #1	18.7 wt %	75.3 wt %	6 wt %
Sample #2	18.5 wt %	74.5 wt %	7 wt %
Sample #3	18.3 wt %	73.7 wt %	8 wt %
Sample #4	18.1 wt %	72.9 wt %	9 wt %
Sample #5	17.9 wt %	72.1 wt %	10 wt %

Table 2. Physical properties of each materials used in this study.

Material	n_e	Δn	Δε
MLC-6657-000	1.6767	0.1702	37.34
RM257	1.687	0.179	−1.5

Electro-optic cells were fabricated by injecting the monomer/ChLC mixtures into an indium-tin-oxide (ITO)-coated glass sandwich cell with a cell-gap of 6 μm and planar alignment (purchased from E. H. C Co., Tokyo, Japan). The helical axis of the ChLC was perpendicular to the glass substrate. The materials were injected into the cell in the isotropic phase (100 °C) and then cooled to 25 °C, at which the sample is in the cholesteric phase, and polymerized by UV light with a wavelength of 365 nm and a power of 200 mW/cm^2 for 40 min. The reflection spectra were measured on a polarizing optical microscope using a fiber-optic spectrometer (Hamamatsu Photonics, PMA-11, Hamamatsu, Japan) with a spectral resolution of 2 nm and a ×10 objective lens, as a square wave electric field with a frequency of 1 kHz was applied along the helical axis on the cell. The response times were also measured under the same

setup with a photomultiplier tube (Hamamatsu, H10722-20, Hamamatsu, Japan) and a digital oscilloscope (Tektronix, TDS 3012, Beaverton, OR, USA). The morphology of the polymer in the nano-composite was observed by scanning electron microscopy (SEM) (Hitachi, S-4300, Tokyo, Japan). After the polymerization process, one of the substrates was removed, and the film was treated by super-critical CO_2 (Rexxam Co. Ltd., SCRD401, Osaka, Japan) to rinse the unpolymerized LC. Gold was coated on the samples for 40 s to form a thin layer approximately 10 nm thick.

3. Results and Discussion

Figure 1 shows the electro-optic characteristics of the polymer/ChLC nano-composite with 8 wt % chiral dopant concentration, before and after polymerization. Before polymerization, the electro-optic response varies depending on the applied field intensity. When a weak electric field is applied, the reflection band becomes narrower and the peak reflectance decreases with increasing electric field. At higher electric fields, the reflection band shifts to shorter wavelengths and eventually disappears. This is explained by the gradual unwinding of the helical structure, showing a transition to the focal-conic state where the helix axis is randomly oriented, before becoming completely unwound [15]. Because the helical structure deforms from a perfect sinusoid, the reflectance decreases compared to the voltage off state. On the other hand, once the material is polymerized, a completely different behavior is observed: above the threshold electric field, the selective reflection band is maintained. In this case, only the long band-edge wavelength shortens, while the short band-edge wavelength remains constant. Because the long and short band-edge wavelengths are given by $\lambda_{long} = n_e \times p$ and $\lambda_{short} = n_o \times p$, the result implies that only the extra-ordinary refractive index decreases, while the ordinary refractive index and pitch remain constant. Unlike the sample before polymerization, the helical structure, stabilized by the crosslinked polymer network, is not destroyed by the electric field. The nano-pores in which the LC molecules are confined are sufficiently small, and so the reorientation of the LC molecules by an electric field affects the effective refractive index without disturbing the macroscopic structure. As the LC molecules reorient along the field, the extra-ordinary refractive index decreases, with the theoretical limit being the value of the ordinary refractive index. The other samples with different chiral dopant concentrations from 6 wt % to 10 wt % also showed similar tendencies.

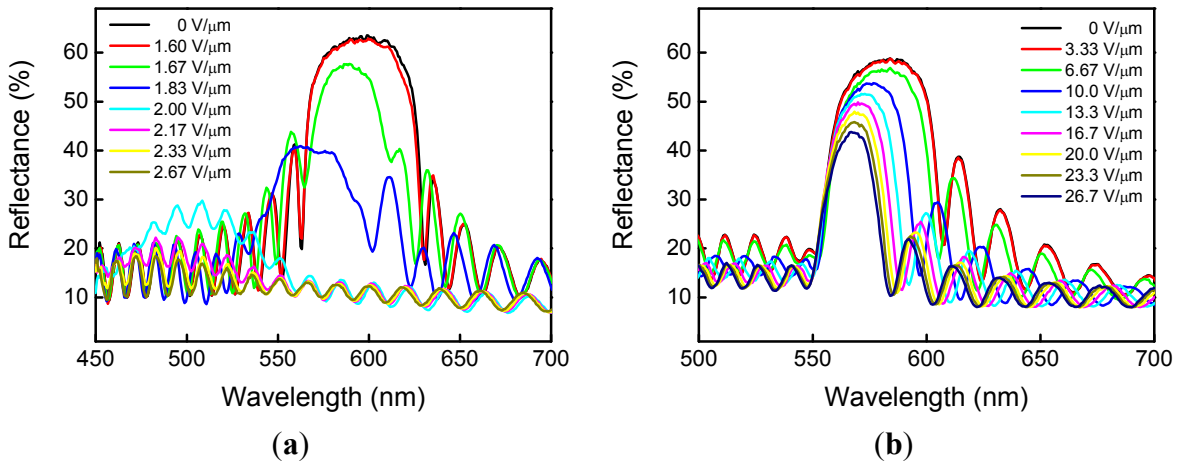

Figure 1. Electro-optic characteristics of the polymer/ChLC nano-composite with 8 wt % chiral dopant concentration (**a**) before polymerization and (**b**) after polymerization.

Figure 2 shows the electric field dependence of the rise and decay times of the polymer/ChLC nano-composite with 8 wt % chiral dopant concentration sample after polymerization. The response characteristics were measured by monitoring the reflected light intensity from the samples, while applying a pulse electric field with a width of 0.5 ms to the cell. The change in the reflected light intensity is caused by the selective reflection band shift. The decay times showed little dependence on the applied electric field, whereas the rise times decreased with increasing electric field. All samples with different chiral dopant concentrations have the same order of decay time (less than 500 μs).

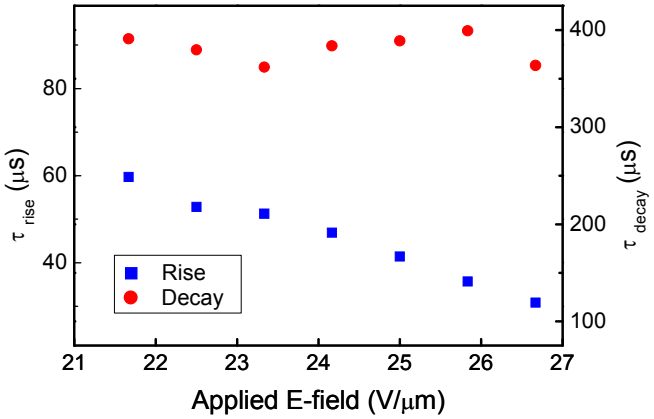

Figure 2. Electric field dependence of the rise and decay times of the polymer/ChLC nano-composite with 8 wt % chiral dopant concentration after polymerization.

Figure 3 shows the reflection images of the photopolymerized polymer/ChLC nano-composite samples under a polarizing optical microscope. The reflected colors of the samples varied as the chiral dopant is increased from 6 wt % to 10 wt %. All images showed that the polymer/ChLC nano-composite samples after polymerization have planar cholesteric structures.

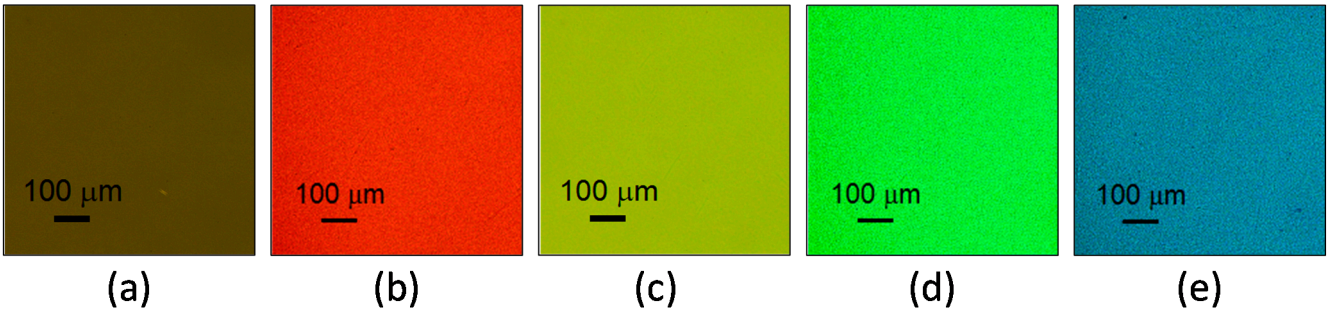

Figure 3. Polarizing optical micrographs of the polymer/ChLC nano-composites after polymerization with different chiral dopant concentrations: (**a**) 6 wt %; (**b**) 7 wt %; (**c**) 8 wt %; (**d**) 9 wt %; (**e**) 10 wt %.

To discuss the helical pitch dependence of the driving voltage, we first show the chiral dopant concentration dependence of the helical pitch. The pitch lengths were measured for samples before and after polymerization to investigate the effect of photopolymerization on the pitch. In a conventional ChLC system, the helical pitch, p, is determined by the helical twisting power, HTP, of the chiral dopant, and its concentration, c; *i.e.*, $p = 1 / (c \times HTP)$ [16]. From this equation, the helical pitch is inversely

proportional to the chiral dopant concentration. Figure 4 shows the dependence of the helical pitch on the chiral dopant concentration in samples before and after polymerization. The Grandjean-Cano wedge method was used for determining the actual helical pitches of the samples [1]. The pitch lengths of the samples both before and after polymerization varied between 273 nm and 458 nm. The solid curves in Figure 4 represent fitting with previous equation. As shown in Figure 4, the helical pitch of the samples, both before and after polymerization, is approximately inversely proportional to the chiral dopant concentration.

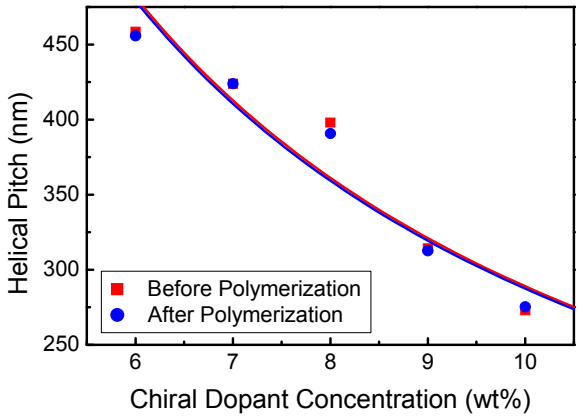

Figure 4. The dependence of the helical pitch on the chiral dopant concentration both before and after polymerization. The red solid squares and blue solid circles are measured results of before and after polymerization, respectively. The red and blue curves are the fitting curves of before and after polymerization, respectively.

The threshold electric field E_{th} of a conventional ChLC is inversely proportional to the helical pitch p, as shown in the following equation,

$$E_{th} = \frac{\pi^2}{p}\sqrt{\frac{K_{22}}{\varepsilon_0 \Delta\varepsilon}} \quad (1)$$

where $\Delta\varepsilon$ is the dielectric anisotropy and K_{22} is the twist elastic constant [17]. This relation implies that the shorter the cholesteric helical pitch, the higher the electrical energy required to unwind the helical structure. To find the threshold field to unwind the helix in the samples before polymerization, we measure the polarized reflectance from the samples and find the electric field at which the reflectance becomes zero; this corresponds to the situation when all molecules are aligned along the electric field and hence shows zero birefringence. Figure 5a shows the polarized reflection intensity integrated over the wavelength 480–730 nm. The reflectance was integrated over the wavelength 480–730 nm since the limited spectral range of the polarizers made it difficult to make the measurement at the central reflection wavelength of each sample. As the chiral dopant concentration increases, or the helical pitch shortens, the threshold electric field increases. Figure 5b shows the threshold electric field with respect to the helical pitch. The solid line in Figure 5b represents fitting with Equation (1). The threshold is approximately inversely proportional to the pitch, as shown in Figure 5b.

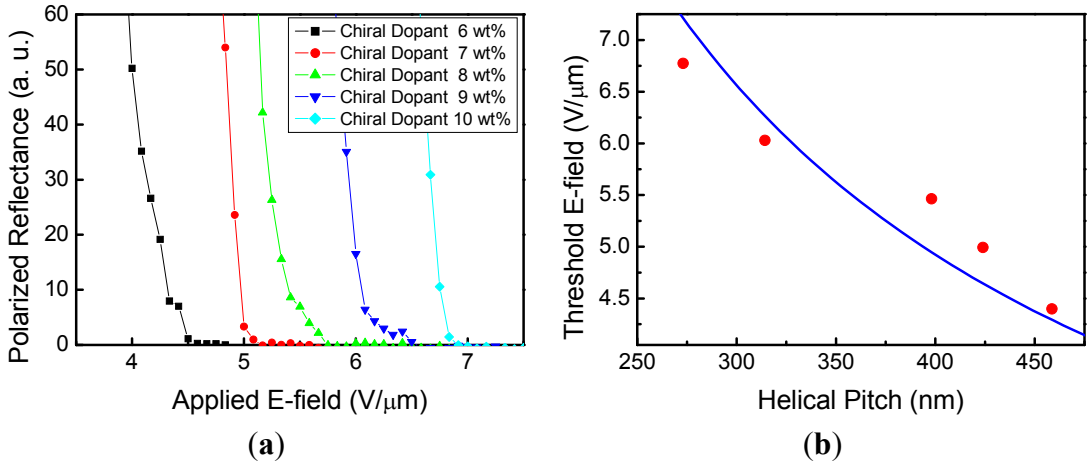

Figure 5. Dependence of the electro-optic response on the chiral dopant concentration of the samples before polymerization. (**a**) Polarized reflection intensity integrated over the wavelength 480–730 nm with respect to the applied electric field at different chiral dopant concentrations; (**b**) Threshold electric field with respect to the helical pitch. The red solid circles are measured results and blue curve is the fitting curve.

Figure 6a shows the applied electric field dependence of the normalized selective reflection band-width after polymerization. The selective reflection band-width is the full width at half maximum of the reflection spectrum, and the normalized selective reflection band-width is defined as the relative band-width compared to the voltage-off state. The threshold electric field is defined as the electric field required for the reflection band to start shifting. In contrast to the unpolymerized samples, the threshold electric field shows little dependence on the helical pitch. As shown in Figure 6b, the thresholds for samples with different helical pitches vary slightly, between 5.5 V/μm and 5.9 V/μm. Consequently, the threshold of the polymer/ChLC nano-composites has no dependence on the helical pitch.

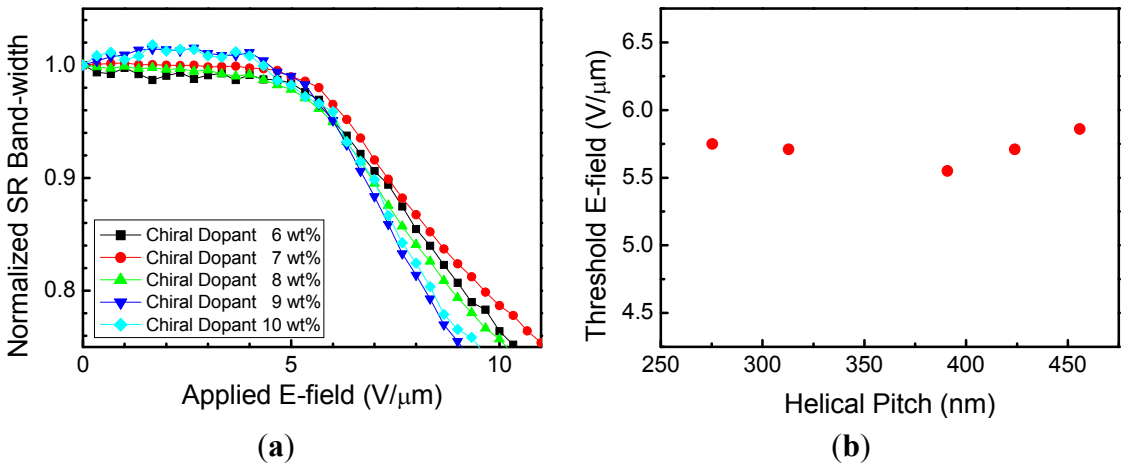

Figure 6. Dependence of the electro-optic response on the chiral dopant concentration of the polymer/ChLC nano-composites after polymerization. (**a**) Normalized selective reflection band-width with respect to the applied electric field at different chiral dopant concentrations; (**b**) Threshold electric field with respect to the helical pitch.

The difference in the pitch dependence of the electro-optic response is most likely attributed to the difference in the driving mechanism. In conventional ChLCs, the threshold is higher for samples with a shorter pitch because of the larger dielectric torque required to unwind the helix [18]. On the other hand, in the polymer/ChLC nano-composite, the helical structure is maintained by the crosslinked polymer networks and only the LC molecules inside the nano-pores orient along the direction of the electric field. The molecules inside the nano-pores experience anchoring along the polymer walls and, this anchoring from the polymer walls, rather than the unwinding of the helix, is the dominant origin of the threshold. In such a case, the threshold varies with the size of the pore rather than the pitch of the helix. In fact, in our previous study, the threshold electric field decreased in the samples having large nano-pores, despite having approximately the same pitch lengths [12].

Figure 7 shows the FE-SEM images of the polymer/ChLC nano-composites with different chiral dopant concentrations after rinsing out the unpolymerized LC with super-critical CO_2. All samples have approximately the same pore-size and polymer network morphology, likely attributed to the fact that the relative concentration of the LC monomer to the nematic LC and the fabrication procedure are the same in all samples. This observation is consistent with our hypothesis that the pore-size is the dominant factor affecting the threshold of polymer/ChLC nano-composites.

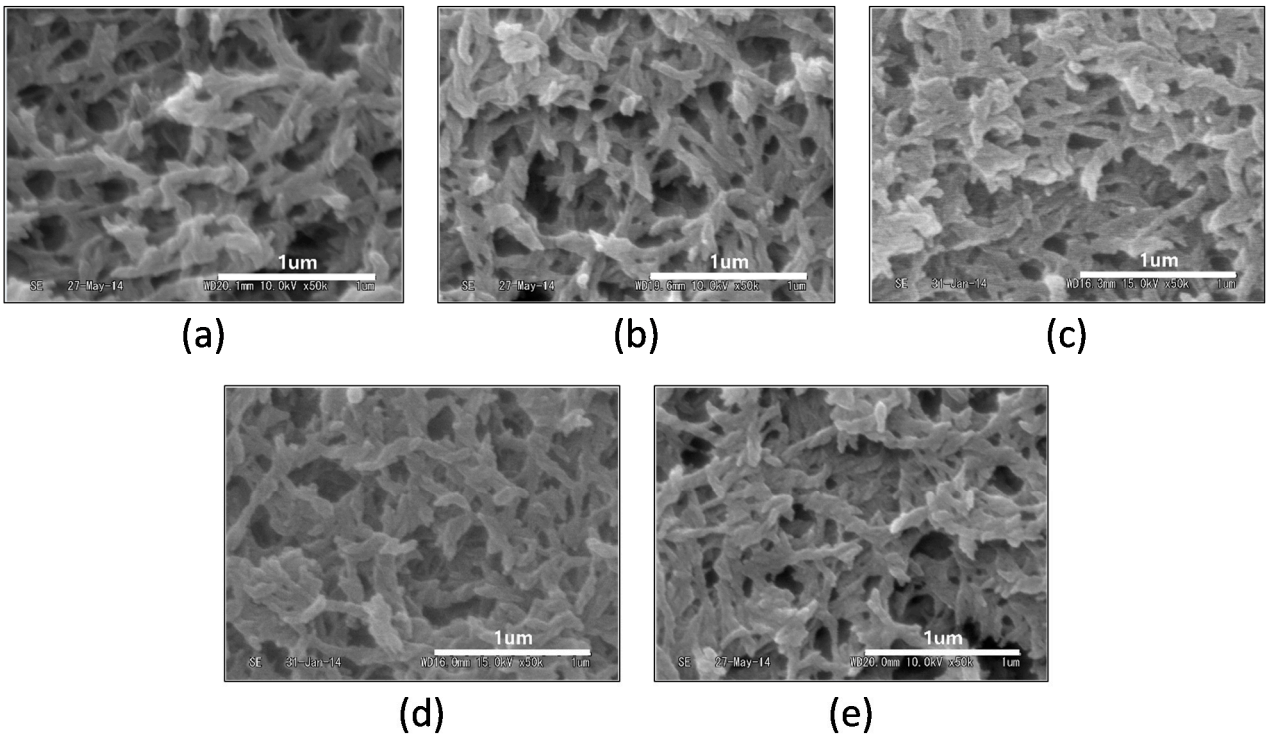

Figure 7. FE-SEM images of the polymer/ChLC nano-composites with different chiral dopant concentrations: (**a**) 6 wt %; (**b**) 7 wt %; (**c**) 8 wt %; (**d**) 9 wt %; (**e**) 10 wt %.

4. Conclusions

The electro-optic properties of polymer/ChLC nano-composites with pitch lengths varying between 273 nm and 458 nm were investigated by spectroscopy and SEM observations. The threshold voltage of the polymer/ChLC nano-composites had no dependence on the helical pitch, in contrast to conventional ChLCs that have a threshold inversely proportional to the helical pitch. The similarity in the polymer

morphology observed in the SEM suggests that the threshold of the nano-composite is determined by the size of the pores in which the LC molecules are confined, rather than the helical pitch. The findings reported here should help realize polymer/ChLC nano-composites with improved electro-optical properties, such as tunable filters and phase modulators.

Acknowledgments

This work was partly supported by KAKENHI(#25630125) and Photonics Advanced Research Center (PARC) at Osaka University.

Author Contributions

H. Kim, H. Yoshida and M. Ozaki designed the experiment and wrote the paper. H. Kim, J. Kobashi and Y. Maeda performed sample fabrication and optical and SEM observations. All authors discussed the results and commented on the manuscript.

Conflicts of Interest

The authors declare no conflict of interest.

References

1. De Gennes, P.G.; Prost, J. *The Physics of Liquid Crystals*, 2nd ed.; Clarendon Press: Oxford, UK, 1993.
2. Choi, S.S.; Morris, S.M.; Huck, W.T.S.; Coles, H.J. Electrically tuneable liquid crystal photonic bandgaps. *Adv. Mater.* **2009**, *21*, 3915–3918.
3. Natarajan, L.V.; White, T.J.; Wofford, J.M.; Tondiglia, V.P.; Sutherland, R.L.; Siwecki, S.A.; Bunning, T.J. Laser initiated thermal tuning of a cholesteric liquid crystal. *Appl. Phys. Lett.* **2010**, *97*, doi:10.1063/1.3459957.
4. Pollmann, P.; Stegemeyer, H. Pressure dependence of the helical structure of cholesteric mesophases. *Chem. Phys. Lett*. **1973**, *20*, 87–89.
5. White, T.J.; Cazzell, S.A.; Freer, A.S.; Yang, D.; Sukhomlinova, L.; Su, L.; Kosa, T.; Taheri, B.; Bunning, T.J. Widely tunable, photoinvertible cholesteric liquid crystals. *Adv. Mater.* **2011**, *23*, 1389–1392.
6. Kang, B.; Choi, H.; Jeong, M.; Wu, J.W. Effective medium analysis for optical control of laser tuning in a mixture of azo-nematics and cholesteric liquid crystal. *J. Opt. Soc. Am. B* **2010**, *27*, 204–207.
7. Yang, D.K.; Doane, J.W.; Yaniv, Z.; Glasser, J. Cholesteric reflective display: Drive scheme and contrast. *Appl. Phys. Lett.* **1994**, *64*, 1905–1907.
8. Yoshida, H.; Lee, C.H.; Matsuhisa, Y.; Fujii, A.; Ozaki, M. Bottom-up fabrication of photonic defect structures in cholesteric liquid crystals based on laser-assisted modification of the helix. *Adv. Mater.* **2007**, *19*, 1187–1190.
9. Inoue, Y.; Yoshida, H.; Inoue, K.; Shiozaki, Y.; Kubo, H.; Fujii, A.; Ozaki, M. Tunable lasing from a cholesteric liquid crystal film embedded with a liquid crystal nanopore network. *Adv. Mater.* **2011**, *23*, 5498–5501.

10. Du, F.; Lu, Y.; Ren, H.; Gauza, S.; Wu, S.-T. Polymer-stabilized cholesteric liquid crystal for polarization independent variable optical attenuator. *Jpn. J. Appl. Phys.* **2004**, *43*, 7083–7086.
11. Sathaye, K.S.; Dupont, L.; de Bougrenet de la Tocnaye, J.-L. Asymmetric tunable Fabry-Perot cavity using switchable polymer stabilized cholesteric liquid crystal optical Bragg mirror. *Opt. Eng.* **2012**, *51*, doi:10.1117/1.OE.51.3.034001.
12. Inoue, Y.; Yoshida, H.; Kubo, H.; Ozaki, M. Deformation-free, microsecond electro-optic tuning of liquid crystals. *Adv. Opt. Mater.* **2013**, *1*, 256–263.
13. Dierking, I.; Kosbar, L.L.; Lowe, A.C.; Held, G.A. Polymer network structure and electro-optic performance of polymer stabilized cholesteric textures I. The influence of curing temperature. *Liq. Crys.* **1998**, *24*, 387–395.
14. Dierking, I.; Kosbar, L.L.; Lowe, A.C.; Held, G.A. Polymer network structure and electro-optic performance of polymer stabilized cholesteric textures II. The effect of UV curing conditions. *Liq. Crys.* **1998**, *24*, 397–406.
15. Hikmet, R.A.M.; Polesso, R. Patterned multicolor switchable cholesteric liquid crystal gels. *Adv. Mater.* **2002**, *14*, 502–504.
16. Wilson, M.R.; Earl, D.J. Calculating the helical twisting power of chiral dopants. *J. Mater. Chem.* **2001**, *11*, 2672–2677.
17. Meyer, R.B. Effects of electric and magnetic fields on the structure of cholesteric liquid crystals. *Appl. Phys. Lett.* **1968**, *12*, 281–282.
18. Yeh, P.; Gu, C. *Optics of Liquid Crystal Displays*, 2nd ed.; Wiley: Hoboken, NJ, USA, 2010.